

# Electric Dichroism Studies on an Aqueous Dispersion of Unilamellar Titanium Oxides: Optical Anisotropy near the Absorption Edge

Hisako Sato,<sup>†,‡</sup> Yoshihisa Hiroe,<sup>†</sup> Takayoshi Sasaki,<sup>‡,§</sup> Kanta Ono,<sup>‡,||</sup> and Akihiko Yamagishi<sup>\*,†,‡</sup>

Department of Earth and Planetary Science, Graduate School of Science, The University of Tokyo, Tokyo 113-0033, Japan, Advanced Materials Laboratory, National Institute for Materials Science, Tsukuba, Ibaraki 305-0044, Japan, and Institute of Materials Structure Science, High Energy Accelerator Research Organization (KEK), Tsukuba, Ibaraki 305-0801, Japan

Received: May 25, 2004; In Final Form: September 2, 2004

Electric dichroism measurements have been performed on an aqueous dispersion of unilamellar titanium oxides produced by the exfoliation of the following three kinds of titanium oxides: (A) lepidocrocite-type titanate ( $\text{Cs}_{0.7}\text{Ti}_{1.825}\square_{0.175}\text{O}_4$ ), (B) tetratitanate ( $\text{K}_2\text{Ti}_4\text{O}_9$ ), and (C) pentatitanate ( $\text{Cs}_2\text{Ti}_5\text{O}_{11}$ ). The AFM images showed that these exfoliated titanium oxides consisted of flakelike particles with an average diameter ranging from 0.1 to 2  $\mu\text{m}$ . Under the applied voltage pulse  $[(1-20) \times 10^3 \text{ V cm}^{-1}]$ , an aqueous dispersion of titanium oxides exhibited orientational dichroism in the UV region with a maximum around 300 nm. From the reduced linear dichroism at complete orientation, the orientation of the effective transition moment ( $\mu_{\text{eff}}$ ) was determined with respect to the oriented axis of a particle. Here  $\mu_{\text{eff}}$  was defined as the vector sum of three orthogonal transition moments of a particle. As a result, an angle ( $\alpha$ ) between  $\mu_{\text{eff}}$  and the oriented axis of a particle was determined to be  $\alpha = 41.6^\circ$ ,  $24.6^\circ$ , and  $23.6^\circ$  at 300 nm for samples A–C, respectively. The results were compared with the recent theoretical calculations of these samples. Electric dichroism was also measured for an aqueous dispersion containing sample A and a cationic molecule,  $[\text{Ru}(\text{phen})_3]^{2+}$ . From the reduced linear dichroism in the visible region, an  $[\text{Ru}(\text{phen})_3]^{2+}$  ion was concluded to be adsorbed with its 3-fold symmetry axis nearly perpendicular to a surface.

## Introduction

Titanium oxide is one of the most extensively studied photoconducting oxides. Its catalytic activity has been attracting wide attention from a practical view for energy conversion, degradation of harmful organic materials, and surface coating.<sup>1–3</sup> Most of the investigations have been done for three-dimensional bulk materials such as anatase and rutile. In contrast to these bulk materials, unilamellar titanium oxides have been synthesized recently by delaminating layered titanates into their single layers.<sup>4,5</sup> Their film properties have been investigated for developing novel types of photocatalytic surface modifiers.<sup>6</sup>

For the application of unilamellar titanium oxides, the electronic properties as a single layer are of essential importance in interpreting the photoresponse of a film. Recently we have performed theoretical calculation on the electronic properties of a single sheet of a titanium dioxide by use of the density functional theory (DFT).<sup>7</sup> The results indicate that the electronic transition moment is dependent on the direction of a crystal axis of a single layer in the wavelength range of 200–400 nm. If this is the case, it is expected that the absorption spectrum of an oriented film exhibits a wavelength-dependent anisotropy.

The present work has been intended to clarify the electronic properties of a single sheet of titanium oxides experimentally. For that purpose, electric dichroism<sup>8,9</sup> was measured for its

aqueous dispersion. According to the method, the induced anisotropy of electronic absorption is detected by aligning an exfoliated layer of titanium oxides in the direction of an electric field. By measuring the magnitude of reduced linear dichroism, it was intended to estimate the anisotropy of electronic absorption of a single sheet.

Besides, electric dichroism was applied to determine the orientation of an adsorbed molecule. This attempt takes advantage of the layer structure of the present material, because such knowledge is difficult to obtain for spherically shaped particles such as anatase or rutile. The results may give a clue to the adsorption structure of a dye molecule on a titanium oxide particle in dye-sensitized solar energy conversion.<sup>2</sup>

## Experimental Section

**Materials.** Precursor layered titanates for three samples examined in this study (A, lepidocrocite-type titanate,  $\text{Cs}_{0.7}\text{Ti}_{1.825}\square_{0.175}\text{O}_4$ ; B, tetratitanate,  $\text{K}_2\text{Ti}_4\text{O}_9$ ; C, pentatitanate,  $\text{Cs}_2\text{Ti}_5\text{O}_{11}$ ) were synthesized according to the methods described previously.<sup>4–6</sup> Briefly, a stoichiometric mixture of alkali-metal carbonates and  $\text{TiO}_2$  was calcinated at 800–1000  $^\circ\text{C}$ . The obtained layered materials were converted into the protonated forms by acid exchange, which were exfoliated by treating them with a tetrabutylammonium hydroxide solution. Aqueous dispersions (ca. 1 g  $\text{L}^{-1}$ ) were stable for several months. A stock solution of each sample was diluted to a concentration of c.a.  $3 \times 10^{-3}$  g  $\text{L}^{-1}$ . Electric resistance was in the order of 20 k $\Omega$  cm. To study the adsorption of a dye by titanium dioxide particles, a cationic molecule,  $[\text{Ru}(\text{phen})_3]^{2+}$ , was used as an adsorbate. Racemic and enantiomeric  $[\text{Ru}(\text{phen})_3](\text{ClO}_4)_2$  were

\* Corresponding author. Tel: +81-3-5841-4546. Fax: +81-3-5841-4553. E-mail: yamagishi@eps.s.u-tokyo.ac.jp.

<sup>†</sup> The University of Tokyo.

<sup>‡</sup> Also at: CREST, Japan Science and Technology Agency.

<sup>§</sup> National Institute for Materials Science.

<sup>||</sup> High Energy Accelerator Research Organization (KEK).

obtained according to the method described previously.<sup>10</sup>  $[\text{Ru}(\text{phen})_3]\text{Cl}_2$  was prepared by refluxing a 1:4 mixture of  $\text{KRuCl}_5(\text{H}_2\text{O})$  and phenanthroline in dimethyl sulfoxide. Resolution was performed by adding the stoichiometric amount of potassium antimonyl tartrate ( $\text{K}_2[\text{SbO}(\text{tart})]_2$ ) to an aqueous solution of  $[\text{Ru}(\text{phen})_3]\text{Cl}_2$ . An insoluble salt,  $\Delta\text{-}[\text{Ru}(\text{phen})_3]\text{-}[\text{SbO}(\text{tart})]_2$ , was eliminated as a precipitate by filtration.  $\Delta\text{-}[\text{Ru}(\text{phen})_3](\text{ClO}_4)_2$  was obtained as a pale yellow solid by adding  $\text{NaClO}_4$  to the filtrate.

**Instrument.** The whole apparatus for electric dichroism measurements consisted of the optical system, the pulse generator, the light detector, and the signal processing system. A monitoring light emitted from a 150 W xenon lamp power supply (Hamamatsu, Japan) was monochromatized through a monochromator. A rotatable polarizer (Glan-Thompson polarizer) was placed between a cell and a photomultiplier. A quartz cell contained two gold-coated electrodes with a distance of 0.4 mm and an optical length of 1.0 cm. An electric field pulse of  $1.0 \text{ ms} \times 0.5\text{--}2 \text{ kV cm}^{-1}$  was applied with a high voltage pulse generator model-60320 (Denkenseiki, Japan). The transient change of transmittance was monitored and stored in a transient oscilloscope (TDS1012 Digital Oscilloscope, Tektronix). To check the correct operation of the instrument, the orientational dichroism of a standard sample containing methylene blue cation ( $1 \times 10^{-5} \text{ M}$ ) and sodium hectorite ( $0.01 \text{ g L}^{-1}$ ) was measured. Figure 1 shows an example, in which the amplitude and sign of a signal at 600 nm depended on the angle ( $\phi$ ) of the polarization of a monitoring light with respect to an electric field according to

$$\Delta A = (A/3)(\Delta\epsilon/\epsilon)(3 \cos^2 \phi - 1) \quad (1)$$

in which  $A$ ,  $\Delta A$ ,  $\epsilon$ , and  $\Delta\epsilon$  denote the isotropic absorbance, the absorbance change induced by imposing an electric field pulse, the isotropic extinction coefficient, and the difference between parallel and vertical extinction coefficients ( $\epsilon_p - \epsilon_v$ ), respectively.<sup>11</sup> The reduced linear dichroism,  $\rho$ , is defined by

$$\rho = (\epsilon_p - \epsilon_v)/\epsilon \quad (2)$$

with  $\epsilon = (1/3)(\epsilon_p + 2\epsilon_v)$ .  $\rho$  at complete orientation,  $\rho_0$ , is obtained by being extrapolated to the infinite field strength. Here,  $\rho_0$  gives us a clue to the direction of a transition moment with respect to the oriented axis of a particle.<sup>11</sup>

The adsorption of a metal complex was measured by centrifuging an aqueous dispersion of titanium oxide and  $[\text{Ru}(\text{phen})_3](\text{ClO}_4)_2$  (1.5 mL) at  $1.2 \times 10^4 \text{ rpm}$  for 1 h. The decrease of  $[\text{Ru}(\text{phen})_3]^{2+}$  was measured from the absorbance change of a supernatant at 450 nm ( $\epsilon_{450} = 2.00 \times 10^4$ ).<sup>10</sup>

**Calculation Method.** Density-functional theory (DFT) calculations presented here were performed using the plane-wave pseudo-potential software CASTEP.<sup>12</sup> The generalized gradient approximation was employed with the Perdew–Burke–Ernzerhof (PBE) functional as an exchange–correlation functional.<sup>13</sup> As for sample A, the structural optimization calculation of unilamellar titanium oxides was performed according to the method as described previously.<sup>7</sup> Electron–core interactions were described by small-core ultrasoft pseudopotentials that were used for both oxygen and titanium.<sup>14</sup> Valence states included 2s and 2p states for O (6 valence electrons), and 3s, 3p, 3d, and 4s states for Ti (12 valence electrons). The smooth parts of the wave functions were expanded in plane-waves with a kinetic-energy cutoff of 800 eV. The Brillouin-zone sampling was performed using a Monkhorst–Pack grid with a  $7 \times 8 \times 2$  grid of  $k$  points.<sup>15</sup> For structural optimization, both the lattice

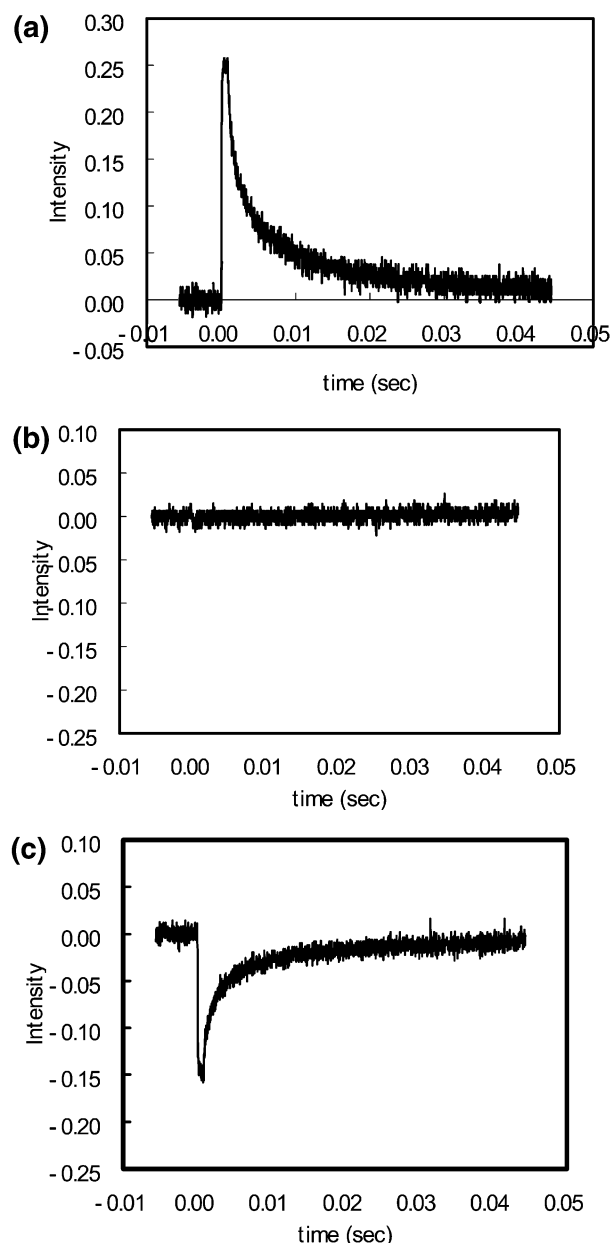


**Figure 1.** Signals of electric dichroism on a standard sample containing methylene blue cation ( $1 \times 10^{-5} \text{ M}$ ) and sodium hectorite ( $0.01 \text{ g L}^{-1}$ ) at 600 nm. The monitoring light was polarized at (a)  $0^\circ$ , (b)  $54.7^\circ$ , and (c)  $90^\circ$  with respect to an electric field direction, respectively.

parameters and coordinates of all atoms were relaxed. Structural optimizations were converged to a displacement of less than 0.0001 nm, and an energy difference of less than  $1 \times 10^{-5} \text{ eV/atom}$  using a Broyden–Fletcher–Goldfarb–Shanno (BFGS) minimization algorithm.

As for samples B and C, the structural parameters were taken from the experimental ones.<sup>16,17</sup> For these samples, no structural optimization was attempted.

## Results

**Electric Dichroism of a Titanium Oxide Dispersion.** The structures of precursor titanates for samples A–C are schematically shown in Figure 2.<sup>16–18</sup> The titanate for sample A crystallizes in an orthorhombic system ( $a = 0.38 \text{ nm}$ ,  $b = 1.72 \text{ nm}$ ,  $c = 0.30 \text{ nm}$ ), whereas the other two crystallize in a monoclinic system ( $a = 1.83 \text{ nm}$ ,  $b = 0.38 \text{ nm}$ ,  $c = 1.20 \text{ nm}$ ,  $\beta = 104^\circ$  for B;  $a = 1.97 \text{ nm}$ ,  $b = 0.38 \text{ nm}$ ,  $c = 1.50 \text{ nm}$ ,  $\beta =$

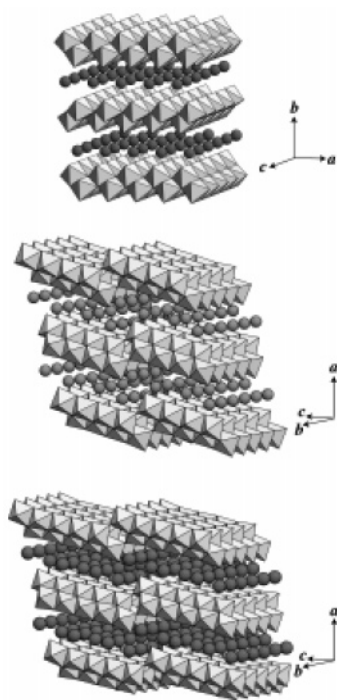


**Figure 2.** Model structures of investigated titanium oxides: (A) lepidocrocite-type titanate  $\text{Cs}_{0.7}\text{Ti}_{1.825}\square_{0.175}\text{O}_4$  (upper),<sup>18</sup> (B) tetratitanate  $\text{K}_2\text{Ti}_4\text{O}_9$  (middle),<sup>16</sup> and (C) pentatitanate  $\text{Cs}_2\text{Ti}_5\text{O}_{11}$  (lower).<sup>17</sup>

107° for C, respectively). In these titanates,  $\text{TiO}_6$  octahedra are combined via edge-sharing to produce corrugated two-dimensional sheets, which accommodate alkali metal ions between them. The sheets in B and C are stepped every 4 and 5 octahedra, respectively. In contrast, the sheet in A is not stepped. The AFM observations of the exfoliated materials revealed that the thickness was 1.0–1.2 nm, clearly showing their unilamellar nature, as shown in Figure 3. The lateral morphology was flakelike with an average diameter of 0.1–2  $\mu\text{m}$ . Sample A tends to have an irregularly square shape whereas samples B and C have needle-like morphology. By referring to the crystal structures in Figure 2, the sheet lateral faces correspond to crystallographic plane of  $a \times c$  for sample A and  $b \times c$  for samples B and C. Particularly, the elongated direction of the latter two samples is parallel to the  $b$  axis.

An aqueous suspension of titanium oxides showed an electronic absorption in the wavelength range of 320–220 nm, as shown in Figure 4. In an isotropic medium, the absorption spectrum has a peak around 260 nm. The transient change of a transmittance was measured on an aqueous dispersion of

**TABLE 1: Orientation of the Effective Transition Moment with Respect to the Aligned Axis of a Particle**

titanium oxide	$\rho_0$	angle (deg) between the effective transition moment and the aligned axis of a particle	
		300 nm	260 nm
A	0.51	41.6	54.7
B	1.14	24.6	54.7
C	1.13	23.6	54.7

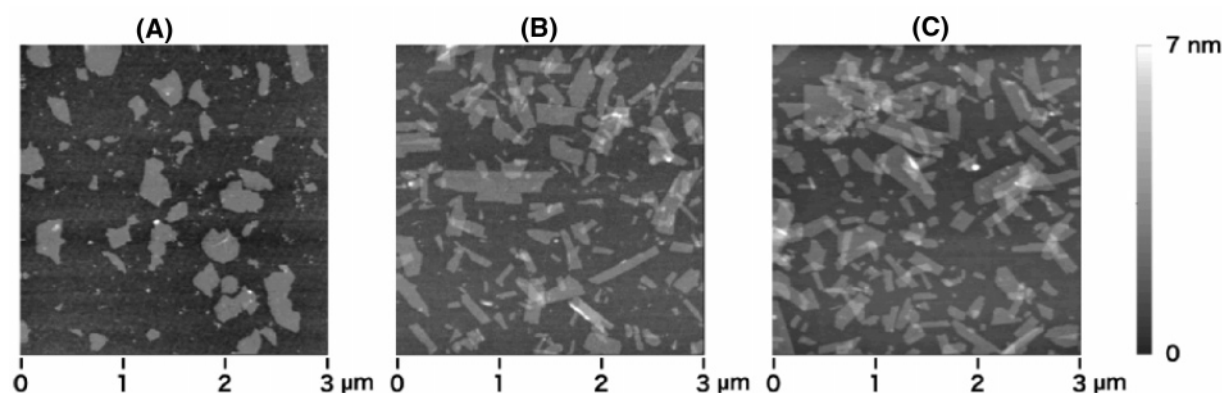
titanium oxide when an electric field pulse was imposed. Figure 5 shows the signals at  $\phi = 0^\circ$ , 54.7° (magic angle), and 90° at 320 nm, respectively. The amplitude of a signal in terms of the change of absorbance ( $\Delta A$ ) obeyed the following equation:

$$\Delta A = (A/3)\rho(3 \cos^2 \phi - 1) + (\Delta A)_0 \quad (\rho = \text{constant}) \quad (3)$$

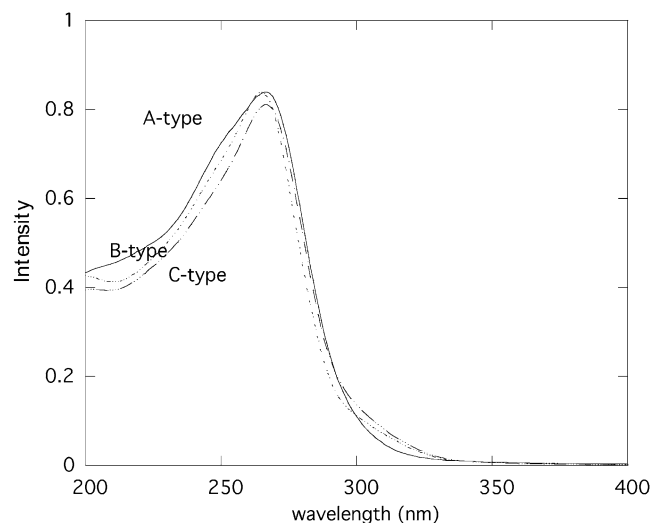
in which  $(\Delta A)_0$  was the induced absorbance change at  $\phi = 54.7^\circ$ . Equation 3 implied that the transient change was an overlap of the orientational dichroism due to the alignment of a titanium oxide particle (the first term in eq 3) and an isotropic absorbance change (the second term in eq 3). As shown by the signals in Figure 5,  $(\Delta A)_0$  relaxed with the same lifetime as those of  $\Delta A$  at  $\phi = 0^\circ$  or 90°. It excludes the possibility that the origin of  $(\Delta A)_0$  was due to the electronic absorbance change induced by the electric field. If that were the case, the change would appear only during the duration of an electric field pulse. Thus one of the possible interpretations for the term  $(\Delta A)_0$  was due to the scattering of the monitoring light. Because the sign of  $(\Delta A)_0$  was minus, the degree of scattering was reduced when the particles aligned under an electric field.

Figure 6a shows the dependence of  $\Delta A - (\Delta A)_0$  on the wavelength at  $\phi = 0^\circ$  for samples A–C, respectively.  $\Delta A - (\Delta A)_0$  at  $\phi = 0^\circ$  had a peak around 300 nm and was nearly zero below 270 nm. These features are quite different from the isotropic spectra of aqueous dispersions for all three samples. The facts implied that, under an aligned state, the UV absorption was isotropic below 270 nm and anisotropic only near the edge of the UV transition. Figure 6b shows the dependence of the reduced linear dichroism ( $\rho = \Delta\epsilon/\epsilon$ ) at 300 nm on the field strength of an electric pulse.  $\rho$  at complete orientation,  $\rho_0$ , was obtained by extrapolating  $\rho$  against the reciprocal of the square of electric field strength (Table 1). The results will be discussed in the proceeding section by comparing with the theoretical calculations.

**Adsorption and Electric Dichroism of  $[\text{Ru}(\text{phen})_3]^{2+}$ .** Figure 7 shows the absorption spectra of  $[\text{Ru}(\text{phen})_3](\text{ClO}_4)_2$  before and after the addition of sample A. On addition of titanium oxides, the band in the wavelength region of 350–



**Figure 3.** AFM images of exfoliated samples of titanium oxides A–C, respectively. The monolayer films were prepared by adsorbing the titanium oxide nanosheets onto a Si wafer chip primed with cationic polymers such as poly(ethylenimine).



**Figure 4.** Electronic absorption spectra of aqueous dispersions of exfoliated titanium oxides: A (solid), B (dotted), and C (broken), respectively. The concentrations were  $4.5 \times 10^{-3} \text{ g L}^{-1}$ .

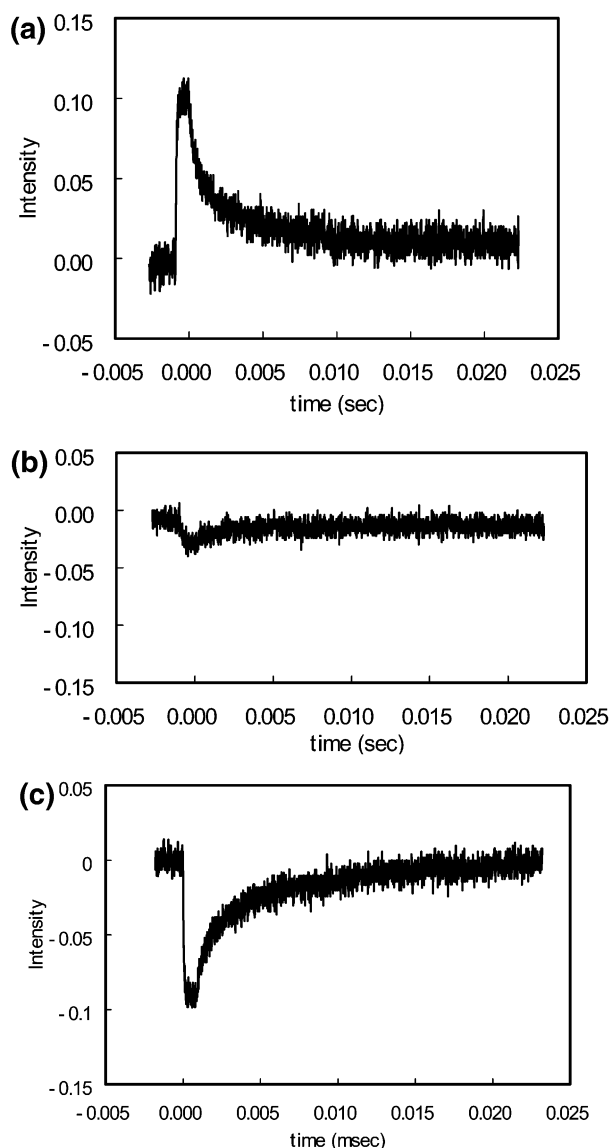


**Figure 5.** Signals of electric dichroism on an aqueous dispersion of exfoliated titanium oxide A ( $2.6 \times 10^{-3} \text{ g L}^{-1}$ ) at 320 nm. The monitoring light was polarized at (a)  $90^\circ$ , (b)  $54.7^\circ$ , and (c)  $0^\circ$  with respect to an electric field direction, respectively.

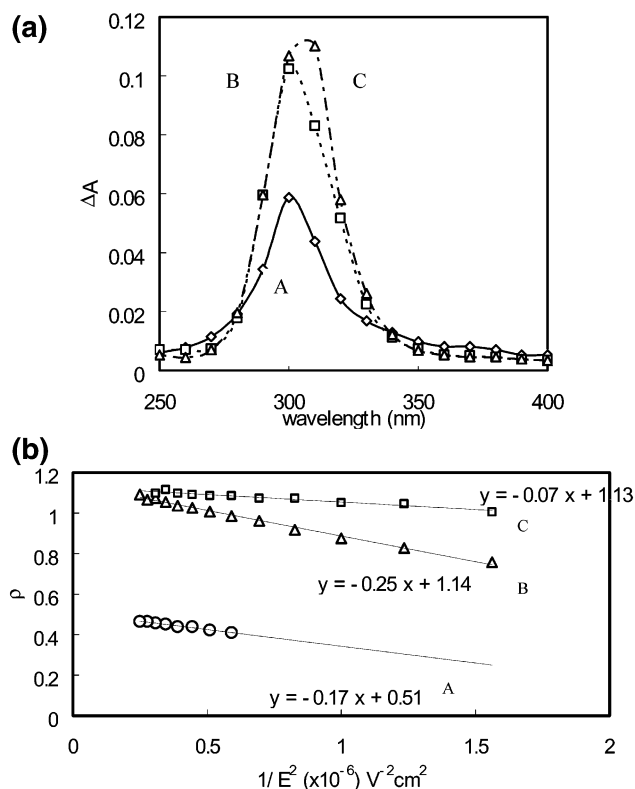


**Figure 6.** (a) Wavelength dependences of the signal amplitude,  $\Delta A - (\Delta A)_0$ , at  $\phi = 0^\circ$  for exfoliated titanium oxide samples A–C. (b) Dependence of reduced linear dichroism,  $\rho$ , on the electric field strength for exfoliated titanium oxide samples A–C.

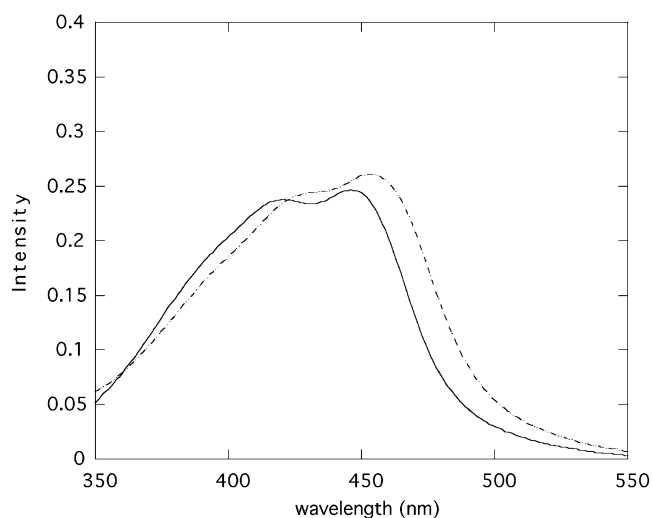


**Figure 7.** Electronic absorption spectra of an aqueous solution of racemic  $[\text{Ru}(\text{phen})_3](\text{ClO}_4)_2$  ( $1.4 \times 10^{-4} \text{ M}$ ) in the absence (solid) and in the presence (dotted) of exfoliated titanium oxide A ( $0.027 \text{ g L}^{-1}$ ).

500 nm was displaced toward the longer wavelength. The change was ascribed to the binding of the cationic complex by a colloiddally dispersed titanium oxide. For both the racemic mixture and enantiomer samples, nearly the same degree of the peak shift toward the longer wavelength (ca. 10 nm) was observed.

The adsorption isotherm of  $[\text{Ru}(\text{phen})_3]^{2+}$  was obtained for sample A. Solid and dotted curves in Figure 8 indicate the results for racemic and enantiomeric  $[\text{Ru}(\text{phen})_3]^{2+}$ , respectively. The maximum adsorption was obtained to be  $(1.3 \pm 0.2) \times 10^{-4} \text{ mol g}^{-1}$  for both samples. The results were contrasted with the previous results on the adsorption by a colloidal clay (sodium



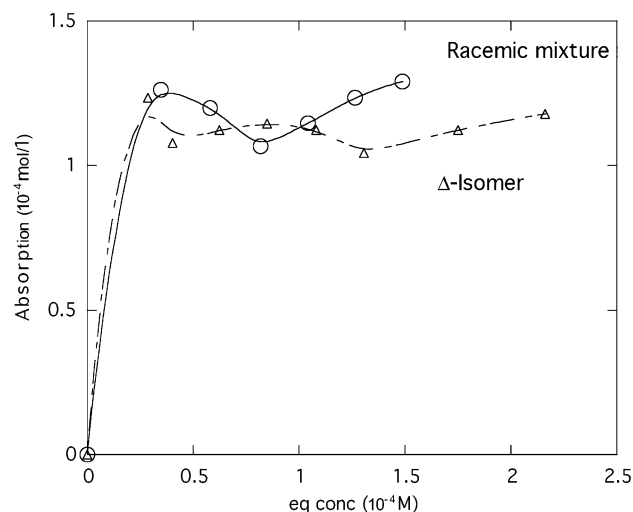


**Figure 8.** Adsorption isotherm of  $[\text{Ru}(\text{phen})_3]^{2+}$  for exfoliated titanium oxide A. Solid and dotted lines are for the racemic mixture and the  $\Delta$ -enantiomer, respectively.

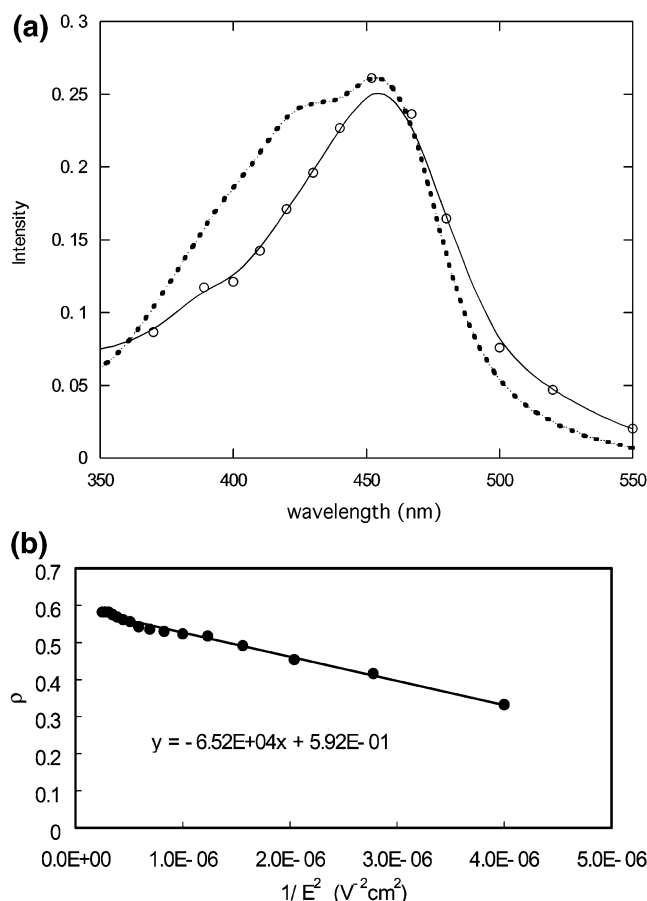


**Figure 9.** (a) Wavelength dependence of the signal amplitude,  $\Delta A$ , at  $\phi = 0^\circ$  for an aqueous dispersion of  $[\text{Ru}(\text{phen})_3](\text{ClO}_4)_2$  and sample A (solid curve). The dotted curve is the isotropic spectrum of the same solution (normalized so as to take the same value at 460 nm). (b) Dependence of reduced linear dichroism,  $\rho$ , on the electric field strength for an aqueous dispersion of  $[\text{Ru}(\text{phen})_3](\text{ClO}_4)_2$  and samples A.

montmorillonite), in which the racemic mixture adsorbs 2 times more than the enantiomer.<sup>19</sup>

Electric dichroism was measured on the sample in which racemic  $[\text{Ru}(\text{phen})_3]^{2+}$  ions were adsorbed by titanium oxide at 3% of the maximum adsorption amount. On imposing an electric field pulse, the transient change of a transmittance was observed in the wavelength region of 300–500 nm where the

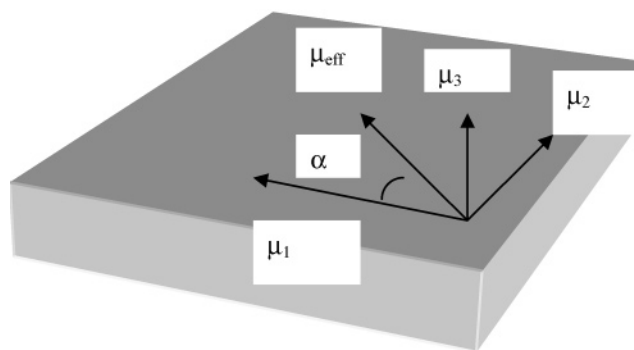


**Figure 10.** Orientations of an effective transition moment ( $\mu_{\text{eff}}$ ) and its three orthogonal components ( $\mu_i$ ).

metal complex showed MLCT (metal-to-ligand charge-transfer) electronic absorption. The dependence of  $\Delta A$  obeyed orientational dichroism as in eq 1 with no isotropic absorbance change induced by the electric field. The wavelength dependence of  $\Delta A$  is shown in Figure 9a. For both A and  $\Delta A$ , the spectra showed the peak around 450 nm, extending their absorption to the wavelength range of 550 nm. The reduced linear dichroism ( $\rho$ ) was extrapolated to the infinite field strength as also shown in Figure 9b.  $\rho$  at complete orientation,  $\rho_0$ , was obtained to be 0.59 at 450 nm.

## Discussion

An aqueous dispersion of titanium oxides showed the transient change of electronic absorption as given in eq 3. The fact implied that an exfoliated layer of titanium oxides oriented in the direction of electric field. Because an exfoliated layer had a platelike shape, each particle was thought to orient with its planar surface in the direction of the electric field. Sample A had an irregular planar shape, which is in  $a \times c$  plane, as described above. Samples B and C were both composed of rectangular-shaped particles, elongated along the  $b$  axis. Thus, under the electric field, the particles were assumed to orient either their  $a$  or  $c$  axis for sample A and their  $b$  axis for samples B and C.

Let a layer have the transition moments of  $\mu_1$ ,  $\mu_2$ , and  $\mu_3$  along the oriented and two normal directions, respectively (Figure 10). Here,  $\mu_2$  and  $\mu_3$  are assumed to be in-plane and out-of-plane components, respectively. Under these assumptions, the observed reduced dichroism at complete orientation is expressed as below:

$$\rho_0 = (\epsilon_1 - \epsilon_2)/\epsilon \quad \text{with} \quad \epsilon = (1/3)(\epsilon_1 + 2\epsilon_2) \quad (4a)$$

$$\epsilon_1 = C\mu_1^2 \quad (4b)$$

$$\epsilon_2 = C(\mu_2^2 + \mu_3^2)\langle \sin^2 \delta \rangle \quad (4c)$$

where  $C$  is a proportional constant and  $\delta$  is the angle of one of the normal axes of an orientated layer with respect to the direction perpendicular to an electric field. Averaging  $\delta$  over  $0-90^\circ$  and expressing  $\mu_1$ ,  $\mu_2$ , and  $\mu_3$  in terms of the effective transition moment,  $\mu_{\text{eff}}$ , which is defined as a vector sum of these three transition moments, is

$$\mu_{\text{eff}}^2 = \mu_1^2 + \mu_2^2 + \mu_3^2 \quad (5)$$

Equation 4a is transformed to

$$\rho_0 = (3/4)(3 \cos^2 \alpha - 1) \quad (6)$$

in which  $\alpha$  represents the angle between  $\mu_1$  and  $\mu_{\text{eff}}$  or  $\mu_1 = \mu_{\text{eff}} \cos \alpha$ .

From the observed values of  $\rho_0$ ,  $\alpha$  is calculated according to eq 6. The results are given in Table 1. Below 260 nm where no absorbance change was induced by an electric field pulse (Figure 6a),  $\rho_0$  was equated to be zero. That is, the electronic absorption was isotropic even in an aligned state. It is proposed that the three components in eq 2 contributed equally to the effective transition moment or  $\mu_1^2 \approx \mu_2^2 \approx \mu_3^2$ . In contrast,  $\rho_0$  had a definite positive value at the absorption edge above 280 nm. From the observed value of  $\rho_0$  at 300 nm,  $\alpha$  was calculated to be 41.6°, 24.6°, and 23.6° for samples A–C, respectively (Table 1). In other words, the effective transition moment at the band edge becomes more parallel with respect to the oriented axis of a particle in the order  $C \approx B > A$ . This may be related to the particle shape of an exfoliated titanate (Figure 2). The irregular shape of sample A may suggest that the crystallite grows in the direction of either the *a* or *c* axis at equal probability. Thus two in-plane transition moments are equal. Besides, if the out-of plane transition moment is smaller than the in-plane transition moments, or  $\mu_1^2 \approx \mu_2^2 \gg \mu_3^2$ ,  $\alpha$  is expected to be around 45°. A crystal of samples B and C grows in the *b* axis. Supposing that the transition moment in this direction was larger than others or  $\mu_1^2 > \mu_2^2, \mu_3^2$ , the effective transition moment would orient toward the orientated axis of a particle.

The above results are compared with the recent calculations on the electronic transitions with respect to crystal axes of unilamellar titanium oxides. Parts A–C of Figure 11 are the results of such calculations, in which the results for sample A are cited from the previous literature.<sup>7</sup> Three main absorptions are predicted at 200, 260, and 300 nm. Although these absorption peaks do not precisely predict the experimental observations, it is noted as a general trend that the absorption at 200 and 260 nm has appreciable contribution from all of the three transition components along the *a*, *b*, and *c* axes or  $\mu_1^2 \approx \mu_2^2 \approx \mu_3^2$ . It implies that the absorption at 200 and 260 nm is nearly isotropic even for a single layer. The absorption above 300 nm has dominantly the in-plane components but little component in the out-of plane direction or  $\mu_1^2 > \mu_2^2 \gg \mu_3^2$ . The edge region of the absorption is confined in the basal plane or of anisotropic nature. These theoretically predicted features are in accord with the experimental observations as given in Table 1.

From the adsorption isotherm of a cationic molecule,  $[\text{Ru}(\text{phen})_3]^{2+}$ , by a colloidal dispersed titanium oxide, the molecule was adsorbed to the maximum adsorption of  $(1.2 \pm 0.2) \times 10^{-4} \text{ mol g}^{-1}$ . Although the plots were scattered, there seemed no difference in the maximum adsorption between the racemic mixture and the enantiomer ( $\Delta$ -isomer). The situations were contrasted with what has been reported on the adsorption of the same molecule by a colloidal clay (sodium montmorillonite).<sup>19</sup> On the surface of a clay mineral crystal, the racemic mixture is adsorbed in excess over the CEC, whereas the enantiomer is adsorbed within the CEC.

The adsorption of  $[\text{Ru}(\text{phen})_3]^{2+}$  by a titanium oxide particle is considered to take place by an ion-exchange mechanism. On the basis of the elemental composition of the present sample A, titanium oxide is calculated to have a cationic exchange capacity (CEC) of  $4.6 \times 10^{-3} \text{ equiv g}^{-1}$ . The observed maximum adsorption corresponded to 5.6% of this CEC. The reason for the fact that the complex cations were not adsorbed to 100% of CEC might be that a titanium oxide particle had already adsorbed cationic ions (or tetrabutylammonium) to an appreciable amount. This cation was used as an exfoliating reagent. Titanium oxide A has a charge density of  $3.1 \text{ e nm}^{-2}$ . Because  $[\text{Ru}(\text{phen})_3]^{2+}$  ions were adsorbed to 5.6% of the CEC,

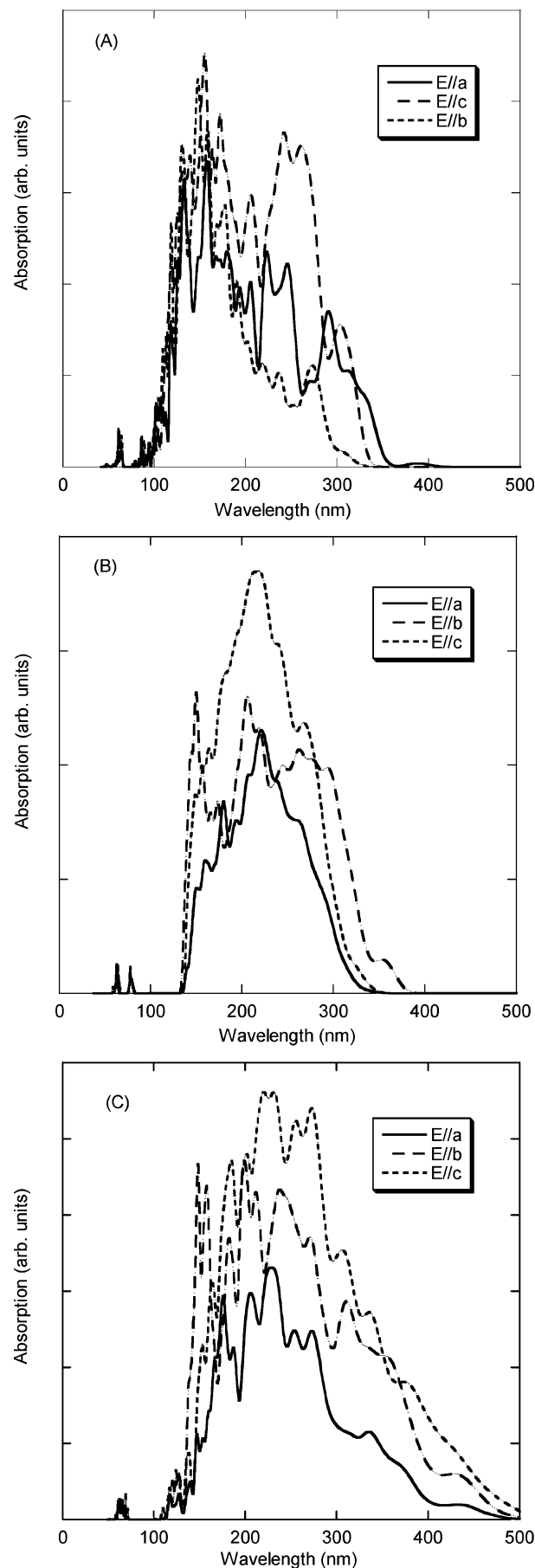


**Figure 11.** Calculated results for the electronic absorbance of titanium oxide samples A–C. Each figure contains three components polarized in the directions of the *a*, *b*, and *c* axes of a unit lattice.

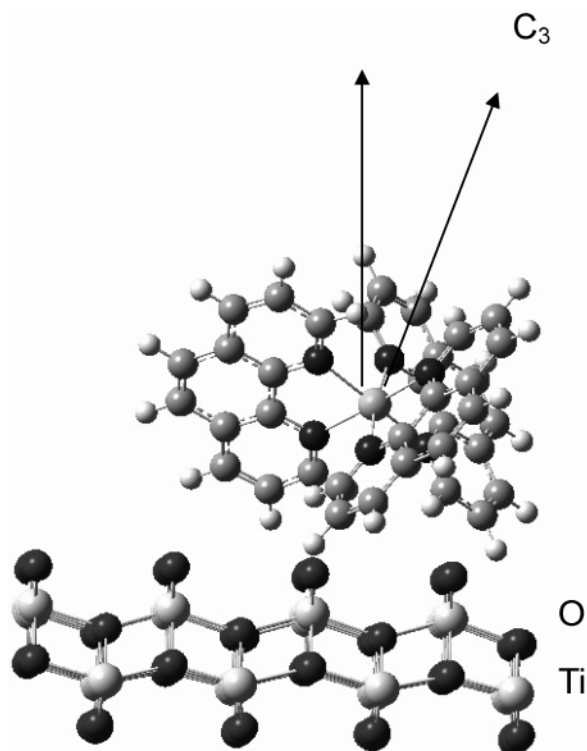


**Figure 12.** Proposed model of  $[\text{Ru}(\text{phen})_3]^{2+}$  adsorbed on a crystallite of titanium oxide. The same results were previously concluded for the adsorption by a clay.<sup>20</sup>

one molecule was estimated to occupy an area of  $11.6 \text{ nm}^2$  at the maximum adsorption. The cross sectional area of  $[\text{Ru}(\text{phen})_3]^{2+}$  is estimated to be  $1.2 \text{ nm}^2$ , when the molecule rotates freely with its  $C_3$  axis perpendicularly to a surface. Thus the molecules are apart from each other even at the maximum adsorption. This is a main reason that there was no chirality effect observed on the adsorption behavior.

The transition moment of  $[\text{Ru}(\text{phen})_3]^{2+}$  is located on a plane perpendicular to the  $C_3$  axis. If the transition moment orients equally on such a plane,  $\rho$  is expressed as<sup>20</sup>

$$\rho = (3/8)(3 \cos^2 \beta - 1) \quad (7)$$

in which  $\beta$  represents the angle of the  $C_3$  axis with respect to the normal to a surface. From  $\rho = 0.59$  at complete orientation,  $\beta$  is determined to be  $22.2^\circ$ . In other words, an adsorbed ion,  $[\text{Ru}(\text{phen})_3]^{2+}$ , was concluded to orient its  $C_3$  axis roughly perpendicularly to a surface. The same results were previously concluded for the adsorption by a clay.<sup>17</sup> If the molecule is regarded as a spheroid, it is expected that the configuration as

shown in Figure 12 corresponds to the most stable one when the molecule is adsorbed dominantly by electrostatic force. Although the same experiment was performed on the adsorption of N3 dye ( $[\text{Ru}(\text{bpy})_2(\text{SCN})_2]$ ), no adsorption took place by the present titanium oxide. The complex was probable to be repelled by the layer of TBA cations preadsorbed by a titanium particle.

In conclusion, the present work has applied the electric dichroism method for a photocatalytic oxide, titanium oxide, to reveal the anisotropic nature of its UV absorption band. As a result, only the edge region of its band has been proved to be anisotropic, in particular, dominated by the in-plane transitions. This is a very initial attempt of the electric dichroism method to the intrinsic transitions of inorganic polymers.<sup>21,22</sup>

**Acknowledgment.** This work has been financially supported by a Grant-in-Aid for scientific Research on Priority Areas (417) from the Ministry of Education, Culture, Sports, Science, and Technology (MEXT) of Japanese Government. Thanks are due to Prof. Sasai (Nagoya University) for his valuable discussion in interpreting electric dichroism results.

## References and Notes

- (1) Fujishima, A.; Honda, K. *Nature (London)* **1972**, 238, 37.
- (2) Bach, U.; Lupo, D.; Comte, P.; Moser, J. E.; Weiss, F.; Salbeck, J.; Spreitzer, H.; Gratzel, M. *Nature* **1998**, 395, 583.
- (3) Wagemaker, M.; Kentgens, A. P. M.; Mulder, F. M. *Nature* **2002**, 418, 397.
- (4) Sasaki, T.; Watanabe, M. *J. Am. Chem. Soc.* **1998**, 120, 4682.
- (5) Sasaki, T.; Ebina, Y.; Kitami, Y.; Watanabe, M.; Oikawa, T. *J. Phys. Chem. B* **2001**, 105, 6116.
- (6) Sasaki, T.; Ebina, Y.; Tanaka, T.; Harada, M.; Watanabe, M. *Chem. Mater.* **2001**, 13, 4661.
- (7) Sato, H.; Ono, K.; Sasaki, T.; Yamagishi, A. *J. Phys. Chem. B* **2003**, 107, 9824.
- (8) Fredericq, E.; Houssier, C. *Electric Dichroism and Electric Birefringence*; Clarendon Press: Oxford, U.K., 1973.
- (9) Naka, K.; Sato, H.; Fujita, T.; Iyi, N.; Yamagishi, A. *J. Phys. Chem. B* **2003**, 107, 8469.
- (10) McCaffery, A. J.; Mason, S. F.; Norman, B. J. *J. Chem. Soc.* **1992**, 114, 10934.
- (11) Dourlent, M.; Hogrel, J. F.; Helen, C. *J. Am. Chem. Soc.* **1974**, 96, 3398.
- (12) Segall, M. D.; Lindan, P. L. D.; Probert, M. J.; Pickard, C. J.; Hasnip, P. J.; Clark, M. C.; Payne, M. C. *J. Phys. Chem.* **2002**, 106, 2717.
- (13) Perdew, J. P.; Burke, K.; Ernzerhof, M. *Phys. Rev. Lett.* **1996**, 77, 3865.
- (14) Vanderbilt, D. *Phys. Rev.* **1990**, B41, 7892.
- (15) Monkhorst, H.; Pack, J. D. *Phys. Rev.* **1976**, B13, 5188.
- (16) Verbaere, A.; Tournoux, M. *Bull. Chim. Soc. Fr.* **1973**, 4, 1237.
- (17) Kwiatkowska, J.; Grey, I. E.; Madsen, I. C.; Bursill, L. A. *Acta Crystallogr.* **1986**, B43, 258.
- (18) Grey, I. E.; Li, C.; Madsen, I. C.; Watts, J. A. *J. Solid State Chem.* **1987**, 66, 7.
- (19) Yamagishi, A.; Soma, M. *J. Am. Chem. Soc.* **1981**, 103, 4640.
- (20) Yamagishi, A. *J. Phys. Chem.* **1981**, 85, 3090.
- (21) Holzheu, S.; Hoffmann, H. *J. Phys. Chem. B* **2002**, 106, 4412.
- (22) Sasai, R.; Sin'ya, N.; Shichi, T.; Takagi, K.; Getto, K. *Langmuir* **1999**, 15, 413.